NJC

Accepted Manuscript

This is an *Accepted Manuscript*, which has been through the Royal Society of Chemistry peer review process and has been accepted for publication.

Accepted Manuscripts are published online shortly after acceptance, before technical editing, formatting and proof reading. Using this free service, authors can make their results available to the community, in citable form, before we publish the edited article. We will replace this *Accepted Manuscript* with the edited and formatted *Advance Article* as soon as it is available.

You can find more information about *Accepted Manuscripts* in the Information for Authors.

Please note that technical editing may introduce minor changes to the text and/or graphics, which may alter content. The journal's standard Terms & Conditions and the Ethical guidelines still apply. In no event shall the Royal Society of Chemistry be held responsible for any errors or omissions in this *Accepted Manuscript* or any consequences arising from the use of any information it contains.

ROYAL SOCIETY OF CHEMISTRY

www.rsc.org/njc

NJC

RSCPublishing

LETTER

Humidity dependency of the thermal phase transition of a cyano bridged Co-W bimetal assembly

Cite this: DOI: 10.1039/x0xx00000x

Noriaki Ozaki,[a] Hiroko Tokoro,[a,b] Yasuto Miyamoto,[a] Shin-ichi Ohkoshi[a,c*]

Received 00th January 2012,
Accepted 00th January 2012

DOI: 10.1039/x0xx00000x

www.rsc.org/

The phase transition of a cyano-bridged Co-W bimetal assembly $Co_3[W(CN)_8]_2$(4-methylpyridine)$_2$(pyridine)$_2{\cdot}xH_2O$ depends on the humidity. This humidity responsivity is attributed to changes in the internal pressure due to the absorption (or desorption) of water molecules in the interstitial sites of the cyano-bridged three-demensional network.

Thermal phase transition phenomena due to charge transfer or spin crossover have received much attention in solid state chemistry.[1,2] Materials exhibiting a phase transition accompanied by a thermal hysteresis loop are especially attractive because they have potential in sensors, displays, and recording media.[2b,3] From this angle, porous coordination polymers or metal-organic frameworks should depend on the environmental conditions.[4] As for magnetic coordination polymers, several types of magnetic materials have been reported, e.g., a humidity-sensitive magnetic material, $Co^{II}[Cr^{III}(CN)_6]_{2/3}{\cdot}zH_2O$;[4d] an alcohol-vapor-sensitive magnetic material, $Cu_3[W(CN)_6]_2$(pyrimidine)$_2{\cdot}8H_2O$;[4e] solvent-sensitive charge-transfer magnetic materials, [Co((*R*)pabn)]-[Fe(tp)(CN)$_3$](BF$_4$)[4i] and [Fe(bpac)*M*(CN)$_4$] (*M*= Pt, Pd, and Ni).[4h]

A series of cyano-bridged Co-W bimetal assemblies,[5] e.g., CsCo[W(CN)$_8$](3-cyanopyridine)$_2{\cdot}H_2O$,[5a,5b] $Co_3[W(CN)_8]_2$-(pyrimidine)$_4{\cdot}6H_2O$,[5c,5d] show thermal phase transitions and photoinduced magnetizations. Such phenomena are driven by a thermally or optically charge-transfer-induced spin transition. Herein we report the humidity sensitivity of $Co_3[W(CN)_8]_2$-(4-methylpyridine)$_2$(pyrimidine)$_2{\cdot}xH_2O$.

The powder-form sample of the present material was prepared according to our previously reported method.[5e] $Cs_3[W^V(CN)_8]$-$\cdot 2H_2O$, $Co^{II}Cl_2{\cdot}6H_2O$, 4-methylpyridine, and pyrimidine, were mixed in aqueous solution (supplementary information §1). Elemental analysis confirmed that the chemical formula of the present compound at 60% relative humidity (RH) was $Co_3[W(CN)_8]_2$(4-methylpyridine)$_2$(pyrimidine)$_2{\cdot}7.5H_2O$: calcd: Co 12.26, W 25.50, C 29.96, H 2.57, N 21.36; found: Co 12.23, W 25.48, C 29.87, H 2.47, N 21.40. The number of water molecules in the sample with RH between 80% and 5% was determined by plotting sample weight as a function of humidity. The number of H_2O molecules (x) decreased from 8.0 to 5.3 as the humidity decreased, but the returned to the initial value as the humidity increased (Fig. 1). The humidity dependence of the IR spectra showed a decrease in the O-H stretching peak at 2800–3700 cm^{-1} (Fig. 2), which is almost consistent with the decrease in the number of H_2O molecules. Although a small spectral change was observed in the CN stretching peak at 2050–2250 cm^{-1}, the change was too small to discuss.

Figure 3 shows the crystal structure refined by Rietveld analysis for the X-ray diffraction (XRD) pattern measured at 80% RH (Fig. S1 and Table S1); the sample had a triclinic crystal structure in the $P\bar{1}$ space group with lattice constants of a = 7.610(1) Å, b = 14.980(2) Å, c = 20.897(8) Å, α = 90.90(8)°, β = 98.34(2)°, and γ = 90.55(2)°. The asymmetric unit consisted of four Co sites (Co1, Co2, Co3, and Co4) and two W sites (W1 and W2). Co (Co1 and Co2) and W(W1 and W2) were bridged by a cyano group, forming

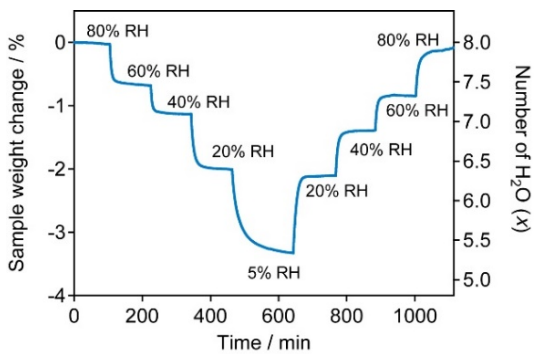

Fig. 1 Humidity dependence of the sample weight change of $Co_3[W(CN)_8]_2$(4-methyl-pyridine)$_2$(pyrimidine)$_2{\cdot}xH_2O$.

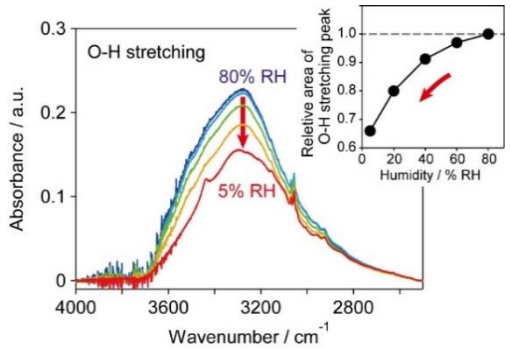

Fig. 2 O-H stretching vibration peak of water in IR spectra of the present sample at 80% RH (blue), 60% RH (light blue), 40% RH (green), 20% RH (orange), and 5% RH (red). (Inset) Plot of the relative peak area of the O-H stretching peak as a function of humidity.

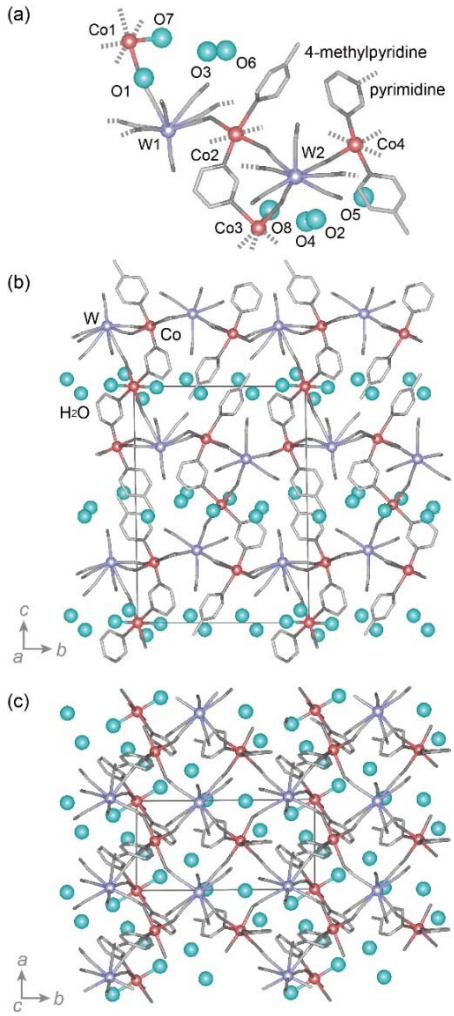

Fig. 3 Crystal structure of the present sample at 80% RH. (a) Asymmetric unit and crystal structure viewed along the (b) *a* and (c) *c* axes. Red, blue, green, gray, and dark gray balls represent Co, W, O, C, and N atoms, respectively.

a two-dimensional grid structure in the *ab* plane. These grid layer were bridged by different Co atoms (Co3 and Co4) and stacked along the *c* axis to construct a three-dimensional network. The interstitial site contained 6.0 molecules of non-coordinated H_2O, while 2.0 H_2O molecules were coordinated to Co. The schematic hydrogen bond network was formed by the coordinated H_2O, non-coordinated H_2O, and CN groups. The refined crystal structure is consistent with the structure reported in our previous paper.[5e]

Successively, the XRD patterns were measured with humidities of 60% RH, 40% RH, 20% RH, and 5% RH. As the humidity decreased, several XRD peaks shifted to a higher angle, but the others did not shift (Fig. 4), indicating an anisotropic lattice contraction. The contractions for the *a*, *b*, and *c* axes from 80% RH to 5% RH were 0.20%, 0.18%, and 0.00%, respectively (Fig. 5 and Table 1). Figures 6a and 6b show the schematic hydrogen bonding networks of the sample at 80% RH and the sample at 5% RH, respectively. Desorption of the water molecules reduced the hydrogen bonding network.

The temperature dependence of the product of molar magnetic susceptibility (χ_M) and temperature (T) ($\chi_M T$–T plot) showed that the present material exhibited a thermal phase transition due to a charge-transfer-induced spin transition (CTIST) from the high-temperature phase [HT phase: Co^{II}_{hs}(S= 3/2)-W^{V}(S= 1/2)] to the low-temperature phase [LT phase: Co^{III}_{ls}(S= 0)-W^{IV}(S= 0)]. Figure7 shows the $\chi_M T$-T plots at 100% RH, 80% RH, 60% RH, 40% RH, 20% RH, and 5% RH. Table S2 lists the transition temperatures ($T_{1/2\downarrow}$ and $T_{1/2\uparrow}$, which are defined as the temperatures

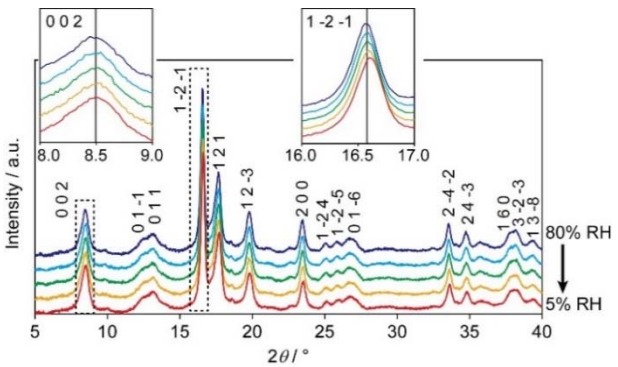

Fig. 4 XRD spectra at 80% RH (blue), 60% RH (light blue), 40% RH (green), 20% RH (orange), and 5% RH (red). Entire spectra and (inset) the peak where a significant shift is not observed (0 0 2) and observed (1 -2 -1).

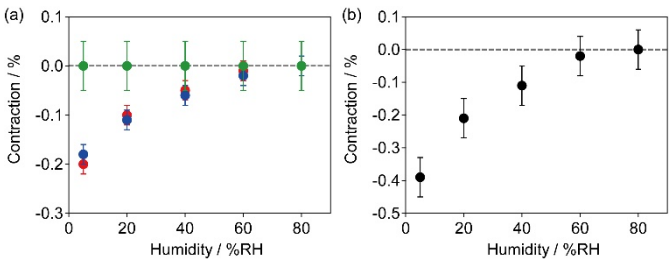

Fig. 5 Plots of contraction of (a) lattice constants and (b) lattice volume as a function of humidity. In (a), red, blue, and green indicate the *a*, *b*, and *c* axis, respectively.

Table 1 Humidity dependence of the lattice constants

	80% RH	60% RH	40% RH	20% RH	5% RH
a / Å	7.610(1)	7.609(1)	7.606(1)	7.602(1)	7.594(1)
b / Å	14.980(2)	14.978(2)	14.970(2)	14.963(2)	14.953(2)
c / Å	20.897(8)	20.897(7)	20.898(8)	20.897(8)	20.897(7)
α / °	90.90(8)	90.95(3)	90.95(3)	90.98(3)	91.06(3)
β / °	98.34(2)	98.33(2)	98.33(2)	98.34(2)	98.37(2)
γ / °	90.55(2)	90.56(1)	90.57(1)	90.58(1)	90.60(1)

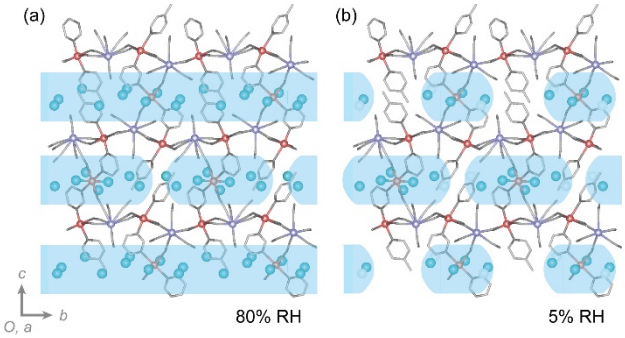

Fig. 6 Schematic illustration of the decrease in the hydrogen bonding network due to desorption of water molecules. Blue shaded areas represent the hydrogen bonding network. Red, blue, green, gray, and dark gray balls represent Co, W, O, C, and N atoms, respectively.

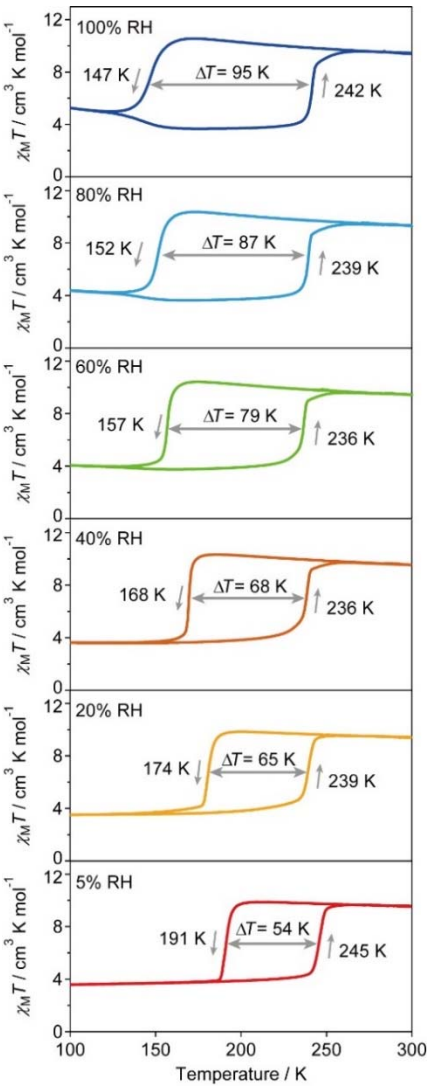

Fig. 7 $\chi_M T$-T plots with a sweeping rate of ±1 K min^{-1} under 5000 Oe of 100% RH (blue), 80% RH (light blue), 60% RH (green), 40% RH (brown), 20% RH (orange), and 5% RH (red).

where the compound has 50% of the population in the HT and LT phases with decreasing or increasing temperature), T_p [$\equiv (T_{1/2\uparrow} + T_{1/2\downarrow})/2$], and ΔT ($\equiv T_{1/2\uparrow} - T_{1/2\downarrow}$) for each humidity. As the humidity decreased, the T_p value increased from 195 K at 100% RH to 218 K at 5% RH and the ΔT value decreased from 95 K at 100% RH to 54 K at 5% RH.

The differential scanning calorimetry (DSC) measurement of the sample in a N_2 atmosphere displayed peak characteristics of a first-order phase transition at 182 K with decreasing temperature and at 238 K with increasing temperature (Fig. S2), which are close to the phase transition temperatures observed in $\chi_M T$-T plots. T_p was 211 K [= (183 K + 238 K)/2], and the estimated transition enthalpy ΔH and transition entropy ΔS were 25.6 kJ mol^{-1} and 116 J K^{-1} mol^{-1}, respectively.

Next the thermal phase transition of the present material was calculated based on the mean-field model of phase transition, Slichter-Drickamer's model.[2a,6] In this model, the Gibbs energy (G) was expressed as $G = \alpha\Delta H + \gamma\alpha(1 - \alpha) + T\{R[\alpha \ln \alpha + (1 - \alpha) \ln (1 - \alpha)] - \alpha\Delta S\}$, where α is the fraction of HT phase, γ is the interaction parameter, and R is gas constant. The DSC measurement was collected in a N_2 atmosphere, and the obtained G was close to the Gibbs energy for the sample at 5% RH. When γ was 9.0 kJ mol^{-1}, the energy minimum disappeared at 189 K with decreasing temperature and at 244 K with increasing temperature (Fig. 8). The calculated HT fraction vs. T plots well reproduced the $\chi_M T$-T plots of the sample at 5% RH.

From the difference of the orbital degeneracy and the spin multiplicity between the HT and LT phases, the spin entropy change ΔS_{spin} (= $R\ln W$, where W is degeneracy of W = 2048/8) in the phase transition for the present system was 46 J K^{-1} mol^{-1} (supplementary information §4). This value was the 40% of the observed ΔS. The remaining 60% was attributed to the phonon mode, which is a reasonable ratio compared to the ratio reported in the spin crossover systems.[2a,2b,7]

In conclusion, this work investigated the humidity dependency of the phase transition behavior in a CoW bimetal assembly, $Co_3[W(CN)_8]_2(4\text{-methylpyridine})_2(\text{pyrimidine})_2{\cdot}xH_2O$. In this humidity dependency, $T_{1/2\downarrow}$ changed more than $T_{1/2\uparrow}$, which is characteristic of changes in the interaction parameter γ. Therefore, the origin of the humidity dependency in the present material was mainly attributed to changes in the internal pressure due to the absorption (or desorption) of water molecules in the interstitial sites of the cyano-bridged Co-W three-dimensional network.

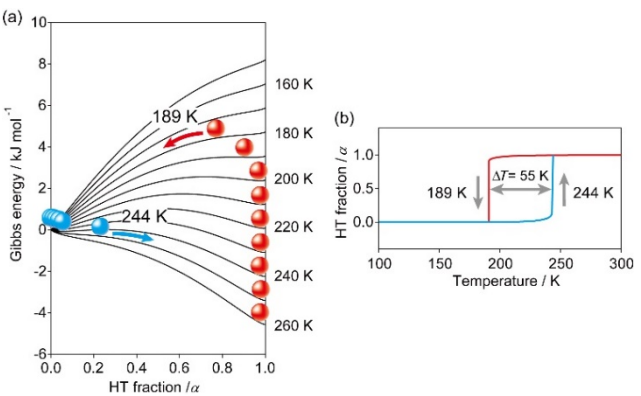

Fig. 8 (a) The temperature dependence of the calculated Gibbs energy as a function of the HT fraction (α) from 260 K to 150 K in 10 K intervals based on the Slichter-Drickamer's model. Red and blue circles indicate the populations of the HT phase and LT phase, respectively. (b) Temperature dependence of the calculated fractions of the HT phase.

Experimental

Synthesis: A powder-form sample of the present material was prepared by adding an aqueous solution of $Cs_3[W^V(CN)_8]\cdot 2H_2O$ to a mixed aqueous solution of $Co^{II}Cl_2\cdot 6H_2O$, 4-methylpyridine, and pyrimidine according to the reported method.[5e]

Physical measurement: The magnetic properties were measured by a superconducting quantum interference device (SQUID) magneto-meter (Quantum Design, MPMS). The IR spectra were recorded by JASCO FTIR-4100 spectrometer using a CaF_2 plate with a scratched surface. The sample-space humidity is controlled by a humidity meter (CTH-1100). For the magnetic properties and IR spectra, the humidity meter was used to monitor the humidity, while the humidity of the sample space was tuned by N_2 gas passed through water. A thermogravimetric system (Rigaku TG-8120) was used to measure the humidity dependence of the sample weight at 293 K. A DSC study was conducted using DSC-8230 (Rigaku). The XRD patterns were measured using a Rigaku Ultima IV with Cu Kα radiation (λ= 1.5406 Å) at 293 K. While measurements, the humidity of the sample space was controlled by a humidity controller (Rigaku HUM-1). Crystallographic data in this paper have been deposited with the Cambridge Crystallographic Data Centre as supplementary publication no. CCDC-836699. Rietveld analyses were performed using RIETAN-FP programs.[8]

Acknowledgements

We are grateful to Dr. Shu Tanaka and Dr. Kosuke Nakagawa for the fruitful discussion. The present research was supported in part by CREST of JST, NEXT from JSPS, a Grant for the GCOE Program 'Chemistry Innovation through Cooperation of Science and Engineering', the Advanced Photon Science Alliance from MEXT, the Asahi Glass Foundation, Izumi Foundation, and Sumitomo Foundation. The authors also recognize the Cryogenic Research Center and the Center for Nano Lithography & Analysis, The University of Tokyo, which are supported by MEXT. Y. M. was supported by JSPS through MERIT. N. O. are grateful for Grant-in-Aid for JSPS fellows.

References

[a] Department of Chemistry, School of Science, The University of Tokyo 7-3-1 Hongo, Bunkyo-ku, Tokyo 113-0033, Japan
[b] NEXT, Japan Society for the Promotion of Science (JSPS), 8 Ichibancho, Chiyoda-ku, Tokyo 102-8472, Japan
[c] CREST, Japan Science and Technology Agency (JST), K's Gobancho,7 Gobancho, Chiyoda-ku, Tokyo 102-0076, Japan

†Electronic Supplementary Information (ESI) available: Results of Rietveld analysis, the atomic coordinates, DSC measurement, Humidity dependence of the transition temperature and thermal hysteresis, and Spin entropy change due to a phase transition. See DOI: 10.1039/c000000x/

1 (a) A. Bleuzen, V. Marvaud, C. Mathonière, B. Sieklucka, and M. Verdaguer, *Inorg. Chem.*, 2009, **48**, 3453. (b) S. Ohkoshi and H. Tokoro, *Acc. Chem. Res.*, 2012, **45**, 1749. (c) N. Shimamoto, S. Ohkoshi, O. Sato, and K. Hashimoto, *Inorg. Chem.*, 2002, **41**, 678. (d) H. Tokoro, S. Ohkoshi, and K. Hashimoto, *Appl. Phys. Lett.*, 2003, **82**, 1245. (e) O. Sato, S. Hayami, Y. Einaga, and Z.-Z. Gu, *Bull. Chem. Soc. Jpn.*, 2003, **76**, 443. (f) S. Ohkoshi, H. Tokoro, T. Hozumi, Y. Zhang, K. Hashimoto, C. Mathonière, I. Bord, G. Rombaut, M. Verelst, C. Cartier dit Moulin, and F. Villain, *J. Am. Chem. Soc.*, 2006, **128**, 270. (g) E. J. Schelter, F. Karadas, C. Avendano, A. V. Prosvirin, W. Wernsdorfer, and K. R. Dunbar, *J. Am. Chem. Soc.*, 2007, **129**, 8139.

2 (a) O. Kahn, *Molecular Magnetism*, VCH, New York, 1993. (b) P. Gütlich and H. A. Goodwin, *Spin Crossover in Transition Metal Compounds I, II, III*, Springer-Verlag, Berlin, 2004. (c) P. Gütlich, A. Hauser, and H. Spiering, *Angew. Chem., Int. Ed.*, 1994, **33**, 2024. (d) P. Gütlich, Y. Garcia, and T. Woike, *Coord. Chem. Rev.*, 2001, **219-221**, 839. (e) S. Decurtins, P. Gütlich, C. P. Köhler, H. Spiering, and A. Hauser, *Chem. Phys. Lett.*, 1984, **105**, 1. (f) J.-A. Real, H. Bolvin, A. Bousseksou, A. Dworkin, O. Kahn, F. Varret, and J. Zarembowitch, *J. Am. Chem. Soc.*, 1992, **114**, 4650. (g) K. Boukheddaden, I. Shteto, B. Hôo, and F. Varret, *Phys. Rev. B*, 2000, **62**, 14796. (h) F. Renz, H. Oshio, V. Ksenofontov, M. Waldeck, H. Spiering, and P. Gütlich, *Angew. Chem., Int. Ed.*, 2000, **39**, 3699. (i) S. Ohkoshi, K. Imoto, Y. Tsunobuchi, S. Takano, and H. Tokoro, *Nat. Chem.*, 2011, **3**, 564. (j) L. Norel, J.-B. Rota, L.-M. Chamoreau, G. Pilet, V. Robert, and C. Train, *Angew. Chem., Int. Ed.*, 2011, **50**, 7128. (k) C. Enachescu, M. Nishino, S. Miyashita, L. Stoleriu, and A. Stancu, *Phys. Rev. B*, 2012, **86**, 054114. (l) T. Q. Hu ng, F. Terki, S. Kamara, M. Dehbaoui, S. Charar, B. Sinha, C. Kim, P. Gandit, I. A. Gural'skiy, G. Molnar, L. Salmon, H. J. Shepherd, and A. Bousseksou, *Angew. Chem., Int. Ed.*, 2013, **52**, 1185. (m) S. Ohkoshi, S. Takano, K. Imoto, M. Yoshikiyo, A. Namai, and H. Tokoro, *Nat. Photonics*, 2014, **8**, 65.

3 O. Kahn and C. Jay Martinez, *Science*, 1998, **279**, 44.

4 (a) A. K. Cheetham, G. Féray, and T. Loiseau, *Angew. Chem., Int. Ed.*, 1999, **38**, 3269. (b) M. Eddaoudi, D. B. Moler, H. Li, B. Chen, T. M. Reineke, M. O'Keeffe, and O. M. Yaghi, *Acc. Chem. Res.*, 2001, **34**, 319. (c) S. Kitagawa, R. Kitaura, and S. Noro, *Angew. Chem., Int. Ed.*, 2004, **43**, 2334. (d) S. Ohkoshi, K. Arai, Y. Sato, and K. Hashimoto, *Nat. Mater.*, 2004, **3**, 857. (e) S. Ohkoshi, Y. Tsunobuchi, H. Takahashi, T. Hozumi, M. Shiro, and K. Hashimoto, *J. Am. Chem. Soc.*, 2007, **129**, 3084. (f) M. Ohba, K. Yoneda, G. Agustí, M. C. Muñoz, A. B. Gaspar, J.-A. Real, M. Yamasaki, H. Ando, Y. Nakao, S. Sakaki, and S. Kitagawa, *Angew. Chem., Int. Ed.*, 2009, **48**, 4767. (g) K. Imoto, D. Takahashi, Y. Tsunobuchi, W. Kosaka, M. Arai, H. Tokoro, and S. Ohkoshi, *Eur. J. Inorg. Chem.*, 2010, **2010**, 4079. (h) C. Bartual-Murgui, L. Salmon, A. Akou, N. A. Ortega-Villar, H. J. Shepherd, M. C. Muñoz, G. Molnár, J.-A. Real, and A. Bousseksou, *Chem. Eur. J.*, 2012, **18**, 507. (i) N. Hoshino, F. Iijima, G. N. Newton, N. Yoshida, T. Shiga, H. Nojiri, A. Nakao, R. Kumai, Y. Murakami, and H. Oshio, *Nat. Chem.*, 2012, **4**, 921.

5 (a) Y. Arimoto, S. Ohkoshi, Z. J. Zhong, H. Seino, Y. Mizobe, and K. Hashimoto, *J. Am. Chem. Soc.*, 2003, **125**, 9240. (b) R. Le Bris, C. Mathonière, and J.-F. Létard, *Chem. Phys. Lett.*, 2006, **426**, 380. (c) S. Ohkoshi, Y. Hamada, T. Matsuda, Y. Tsunobuchi, and H. Tokoro, *Chem. Mater.*, 2008, **20**, 3048. (d) R. Le Bris, Y. Tsunobuchi, C. Mathonière, H. Tokoro, S. Ohkoshi, N. Ould-Moussa, G. Molnar, A. Bousseksou, and J.-F. Létard, *Inorg. Chem.*, 2012, **51**, 2852. (e) N. Ozaki, H. Tokoro, Y. Hamada, A. Namai, T. Matsuda, S. Kaneko, and S. Ohkoshi, *Adv. Funct. Mater.*, 2012, **22**, 2089.

6 (a) C. P. Slichter and H. G. Drickamer, *J. Chem. Phys.*, 1972, **56**, 2142. (b) S. Ohkoshi, Y. Tsunobuchi, T. Matsuda, K. Hashimoto, A. Namai, F. Hakoe, and H. Tokoro, *Nat. Chem.*, 2010, **2**, 539.

7 M. Sorai, *Bull. Chem. Soc. Jpn.*, 2001, **74**, 2223.

8 F. Izumi, K. Momma, *Solid. State. Phenom.*, 2007, **15**, 130.

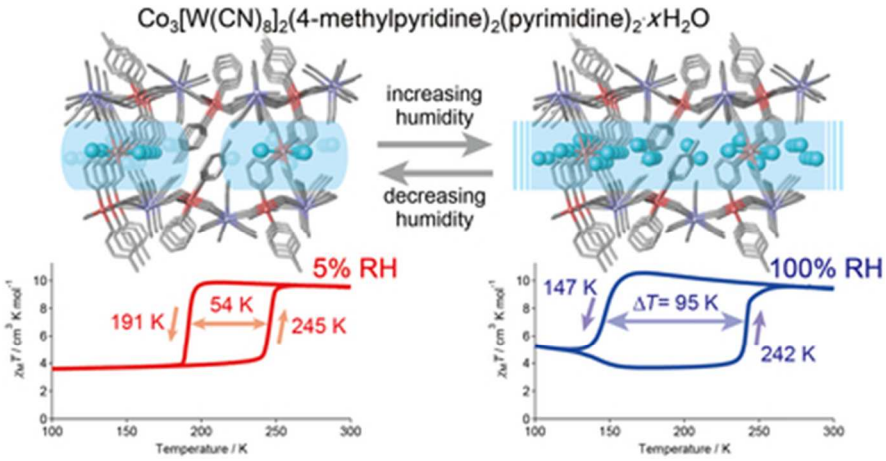

A three-dimensional cyano-bridged Co-W bimetal assembly shows the humidity-dependent phase transition due to desorption or absorption of water molecules.
37x19mm (300 x 300 DPI)